Supplemental Material

p120-catenin is an obligate haploinsufficient tumor suppressor in intestinal neoplasia

***Sarah P. Short, *Jumpei Kondo, Whitney G. Smalley-Freed, Haruna Takeda3, Michael R. Dohn, Anne E. Powell, Robert H. Carnahan, Mary K. Washington, Manish Tripathi, D. Michael Payne, Nancy A. Jenkins, Neal G. Copeland, Robert J. Coffey, Albert B. Reynolds**

Genotype	# of Tumors	Score (Mean ± SD)
Apc$^{1638N/+}$	8	2.38 ± 0.52
Apc$^{1638N/+}$; p120 KO	35	1.09 ± 0.28

Supplemental Table 1. Tumors from *Apc*$^{1638N/+}$; *p120*$^{f/f}$; *Villin*^{CreERT2} mice treated with corn oil (*Apc*$^{1638N/+}$) or tamoxifen (*Apc*$^{1638N/+}$; p120 KO) were labelled by immunofluorescence with specific p120 antibodies and the signal intensity estimated on a scale of 0 – 4. Scoring: 0= complete p120 KO, 4 = WT p120 staining. Scores are shown as the mean ± standard deviation. *P* =0.043, unpaired Student's t-test.

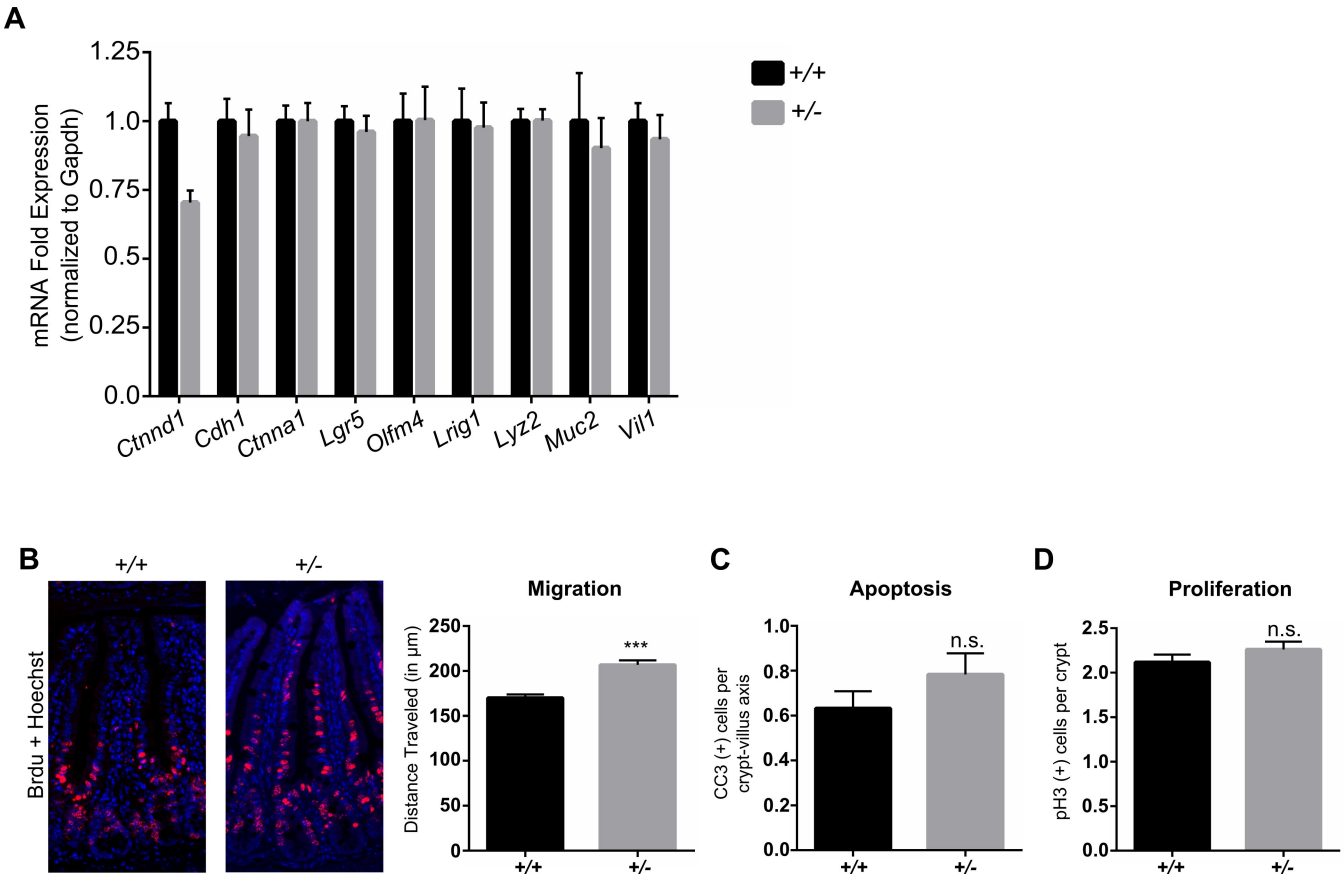

Supplementary Figure 1. Intestinal homeostasis is not obviously altered by p120 heterozygosity. **(A)** qRT-PCR analysis of small intestinal samples from littermate $p120^{+/+}$ (+/+) and $p120^{+/-}$ mice (+/-) (*n*=5 mice per genotype). While p120 (*Ctnnd1*) is decreased, no change in stem cell or differentiation markers was observed. **(B)** p120 WT (+/+) and heterozygous (+/-) mice were injected with BrdU and sacrificed 36 hours treatment. Distance of migrated BrdU (+) cells was measured by Metamorph software and quantified (right, ***P<0.001, unpaired Student's t-test). (**C**) Quantification of FFPE staining for apoptotic marker cleaved caspase 3 (CC3) and **(D)** cell proliferation marker phospho-histone H3 (pH3). Among these experiments, a small increase in the rate of crypt – villus cell migration was the only significant alteration (*n*=5 mice and ~20 crypt/villus units

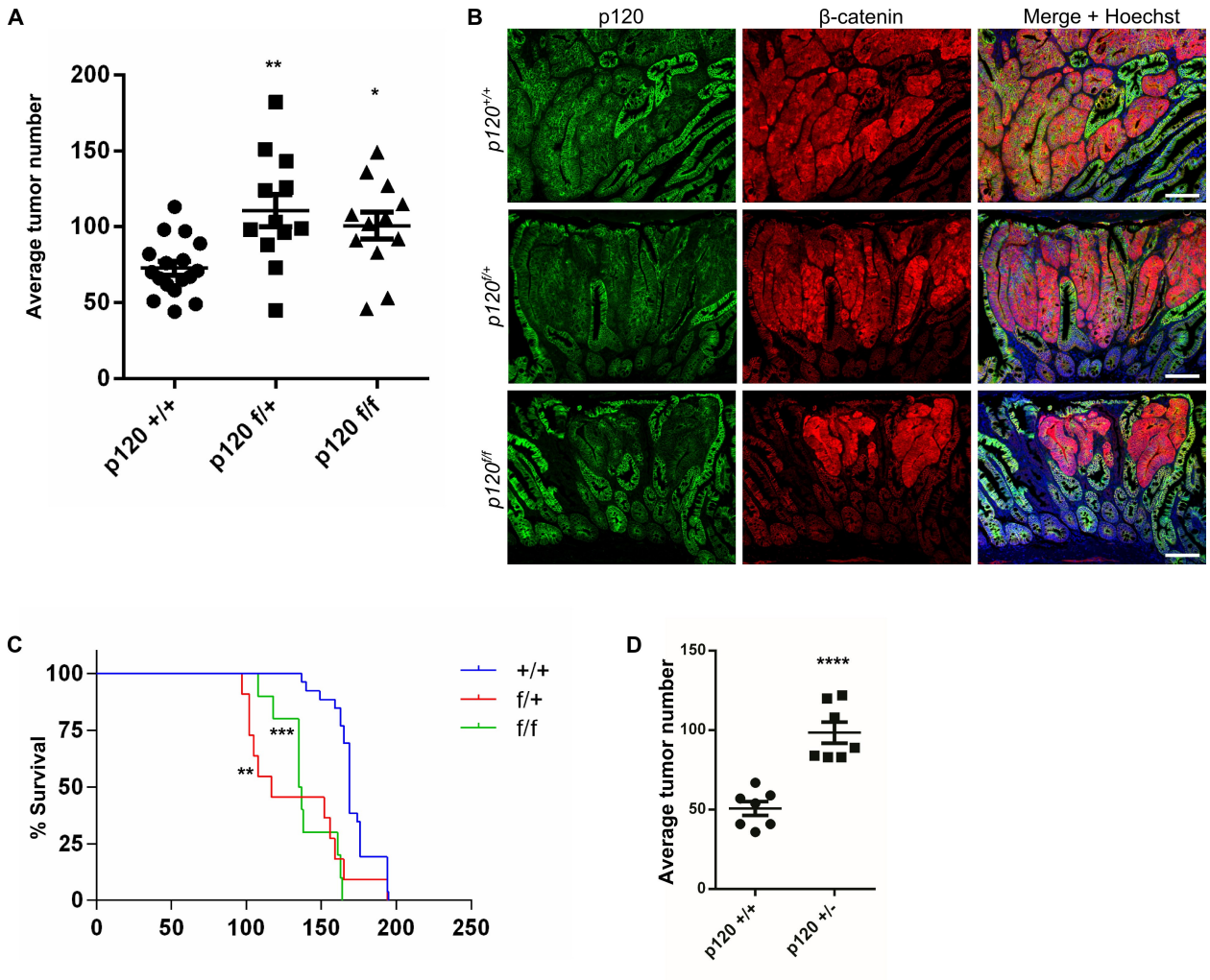

Supplemental Figure 2. The tumorigenic consequences of p120 haploinsufficiency are not obviously linked to potential microenvironmental alterations (e.g., inflammation) associated with limited p120 ablation. **(A)** *Apc*$^{Min/+}$; *Villin*^{CreERT2} mice were crossed with p120 floxed mice to yield *p120*$^{+/+}$, *p120*$^{f/+}$, *p120*$^{f/f}$ cohorts (*n*=16 *p120*$^{+/+}$, 12 *p120*$^{f/+}$, and 12 *p120*$^{f/f}$). The *p120*$^{f/+}$ cohort, which eliminates unanticipated side effects emanating from p120 null cells, was essentially indistinguishable from *p120*$^{f/f}$ groups (*p120*$^{+/+}$, 72.8±5.1; *p120*$^{f/+}$, 110.7±11.6; *p120*$^{f/f}$, 100.1±11) (**P*<0.05, ***P* < 0.01 versus *p120*$^{+/+}$ cohort, one-way ANOVA pairwise comparisons with Tukey's correction, *p120*$^{f/+}$ vs. *p120*$^{f/f}$ nonsignificant). **(B)** Representative tumors from each genotype immunostained for p120 (green) and β-catenin (red). Scale bar, 200μm. **(C)** Decreased survival of *p120*$^{f/+}$ (***P* < 0.01) and *p120*$^{f/f}$ cohorts (****P* < 0.001, Log-rank test) as compared to WT. **(D)** *Apc*$^{Min/+}$ mice were crossed with p120 heterozygous mice to yield *p120*$^{+/+}$ and *p120*$^{+/-}$ *Apc*$^{Min/+}$ cohorts, enabling comparison of haploinsufficiency with no other variables (*n*=7 mice per group). Tumor numbers for *Apc*$^{Min/}$; *p120*$^{+/-}$ and *Apc*$^{Min/+}$; *p120*$^{+/+}$ littermate controls (98.3±6.6 vs. 50.7±4.3, *****P* < 0.001, unpaired Student's t-test) are shown. Error bars on all graphs represent SEM.

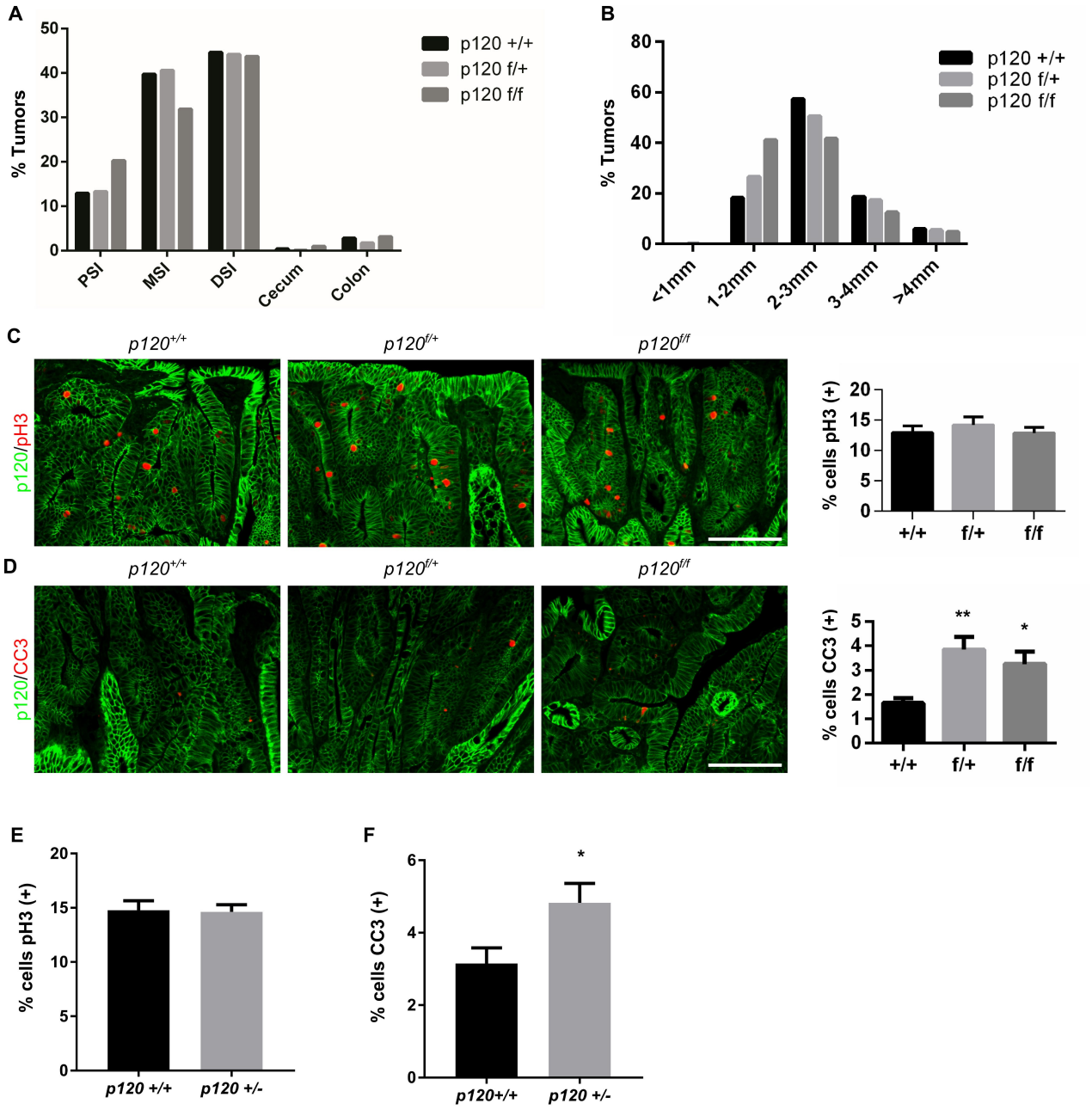

Supplemental Figure 3. Increased apoptosis associated with monoallelic p120 loss. **(A)** Intestines from *Apc*^{Min}; *Vil-CreER*; *p120 floxed* mice were divided into the proximal (PSI), middle (MSI), and distal (DSI) small intestine, cecum, and colon. Limited p120 KO did not affect tumor distribution in *p120*$^{f/+}$ and *p120*$^{f/f}$ cohorts. **(B)** Tumor size was measured by caliper in *Apc*^{Min}; *Vil-CreER*; *p120 floxed* mice. **(C)** Tumor samples were immunolabeled for cell proliferation marker phospho-histone H3 (pH3, left) and the results quantified (right, *n*=25 high powered fields per group). **(D)** Tumor samples were immunolabelled for apoptotic marker cleaved caspase 3 (CC3, left) and the results quantified (right, *n*=25 high powered fields per group). Apoptosis was significantly elevated in the *p120*$^{f/+}$ and *p120*$^{f/f}$ cohorts. (**P*<0.05, ***P*<0.01 vs *p120*$^{+/+}$ group, one-way ANOVA pairwise comparisons with Tukey's correction, *p120*$^{f/+}$ vs. *p120*$^{f/f}$ nonsignificant). Scale bar, 100µm. **(E)** Cell proliferation was measured in *Apc*$^{Min/+}$; *p120*$^{+/-}$ and *Apc*$^{Min/+}$; *p120*$^{+/+}$ (control) animals by pH3 immunostaining. **(F)** Increased apoptosis (CC3 staining) associated with monoallelic p120 ablation in *Apc*$^{Min/+}$ mice (**P*< 0.05, unpaired Student's t-test). Error bars on all graphs represent SEM.

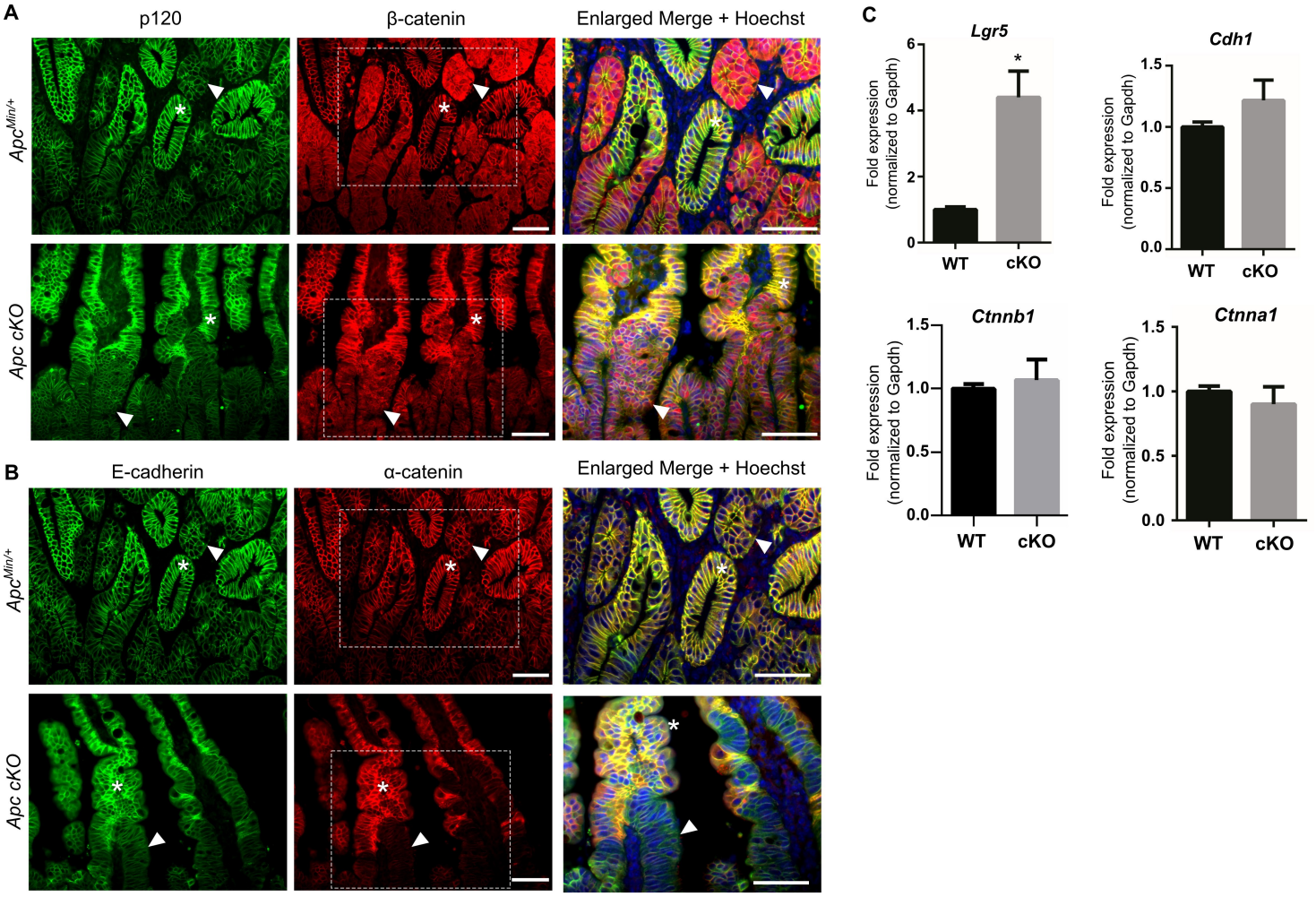

Supplemental Figure 4. p120, E-cadherin, and α-catenin co-localize and vary together in response to changes in *Apc* status. **(A)** Serial sections from FFPE samples of an $Apc^{Min/+}$ intestinal adenoma (top panels) or small intestinal tissue from an *Apc* cKO mouse 3 days post-tamoxifen treatment (lower panels) were co-stained for p120 and β-catenin or **(B)** E-cadherin and α-catenin. p120, E-cadherin and α-catenin colocalize and their levels vary in sync under all conditions, including WT (*) and *Apc*-ablated tumor and cKO tissue (arrowhead), indicating that the E-cadherin complex remains intact regardless of staining intensity. β-catenin levels, on the other hand, can be independently controlled by events impacting the canonical Wnt pathway (e.g., *Apc*-LOH) leading to staining that varies inversely to that of the other core cadherin components. Boxes represent area enlarged. Scale bar, 100μm. **(C)** qRT-PCR analysis of *Apc* cKO intestine samples show elevated *Lgr5* expression, consistent with constitutive Wnt activation, while mRNAs encoding the cadherin complex components are unchanged (n=5 mice per group). Error bars represent SEM (*P<0.05, unpaired t-test with Welch's correction).

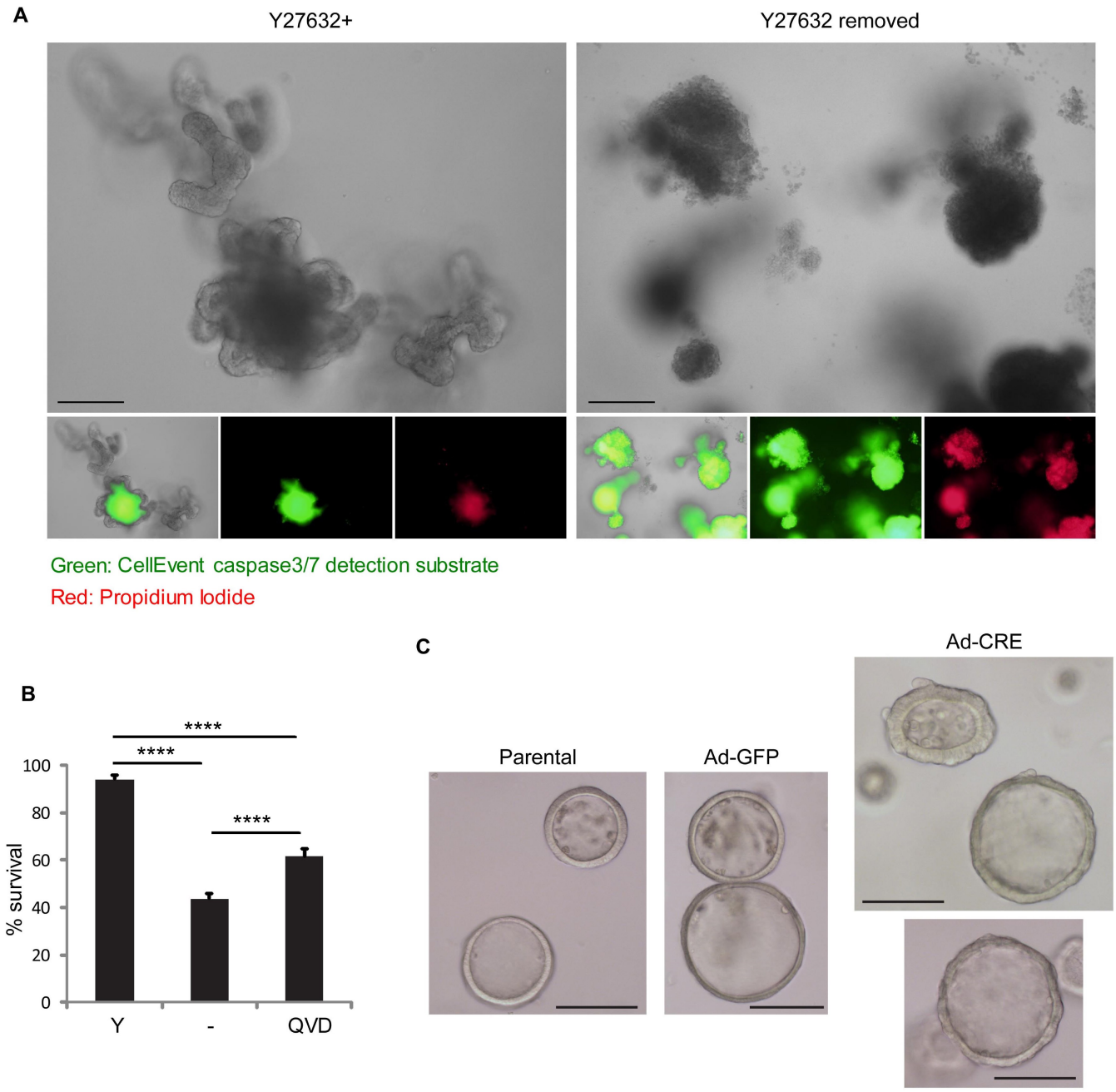

Supplementary Figure 5. Biallelic p120 loss induces cell death in *Apc*$^{Min/+}$ tumor organoids. **(A)** Representative images of *Apc*^{Min}*; p120*$^{f/f}$ small intestinal tumor organoids infected with Adeno-CRE virus cultured with or without Y27632. Note that organoids cultured with Y27632 are translucent with smooth surfaces, while organoids cultured without Y27632 are dark with dispersed cells. Non-Y27632 treated organoids are widely positive for both caspase3/7 activity (detected by CellEvent Caspase-3/7, green) and propidium iodide (red), while organoids with Y27632 have dead cells only in the lumen where differentiated cells are shed. Scale bar, 100µm. **(B)** Quantified viability of *Apc*$^{Min/+}$*; p120*$^{f/f}$ tumor organoids infected with Adeno-CRE virus. Viability was evaluated after 5 days of culture with Y27632 (Y, 10µM), without Y27632 (-), or with the pan caspase inhibitor Q-VD-OPh (QVD, 50µM). Data is shown as mean ± SEM of 4 cultures for each condition (~200 organoids per culture). (****P<0.0001, one-way ANOVA pairwise comparisons with Tukey's correction). **(C)** Representative images of *Apc*$^{Min/+}$*; p120*$^{f/f}$ tumor organoids with cystic morphology for p120-KO (Ad-CRE) and control (Parental and Ad-GFP) organoids. Scale bar, 100µm.

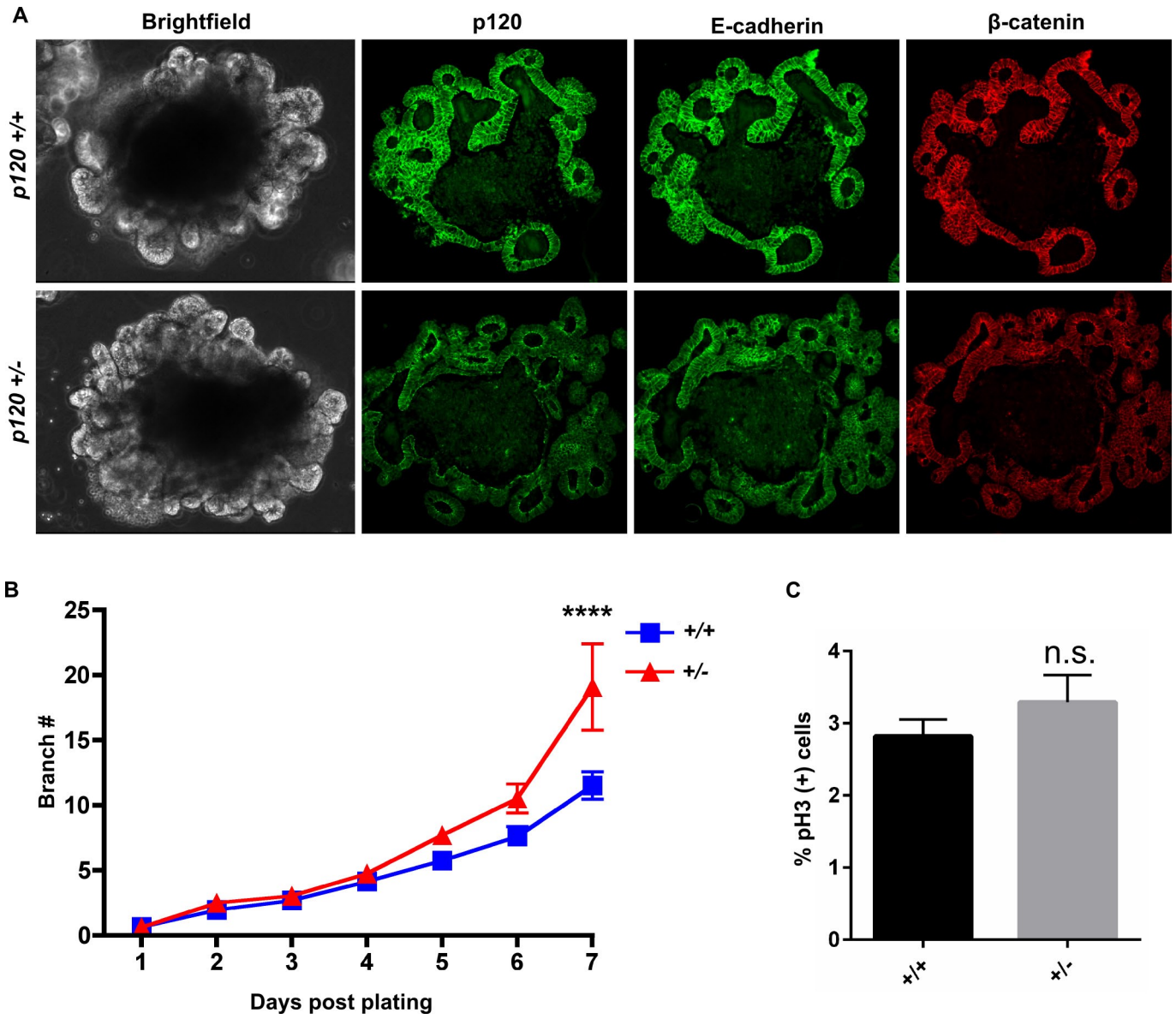

Supplementary Figure 6. Increased branching associated with monoallelic p120 ablation in small intestinal enteroids. **(A)** Representative bright-field images from *p120*$^{+/+}$ and *p120*$^{+/-}$ small intestinal enteroids (far left), and immunofluorescence-labelled versions thereof: p120 (middle left), E-cadherin (middle right), and β-catenin (far right). Note more complex branching structure and decreased staining intensity in *p120*$^{+/-}$ samples. **(B)** Small intestinal enteroids were sheared to single buds and branch number was quantified daily over 7 days (n > 60 organoids per genotype per time point) (Day 7, ****P<0.0001, two-way ANOVA with Sidak's multiple comparison test). Results representative of 3 independent experiments. **(C)** Monoallelic p120 ablation did not significantly alter organoid cell proliferation rates (as measured by pH3 staining). Error bars represent SEM. n.s., nonsignificant, Student's t-test.

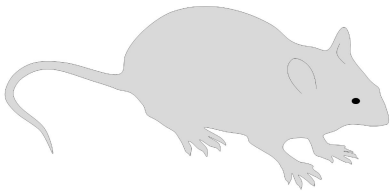

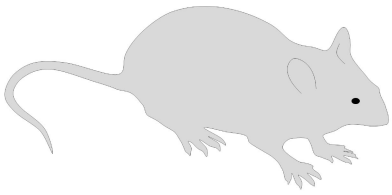

LSL-SB11 (neo/neo); T2/Onc2 (Tg/Tg) **X** **Sensitizing mutant (mut/+); Vil-CreERT2**

1) LSL-SB11 (neo/+); T2/Onc2 (Tg/+); LSL-K-ras$^{(G12D/+)}$; Vil-CreERT2

2) LSL-SB11 (neo/+); T2/Onc2 (Tg/+); Smad4$^{(fl/+)}$; Vil-CreERT2

3) LSL-SB11 (neo/+); T2/Onc2 (Tg/+); p53$^{(R172H/+)}$; Vil-CreERT2

Supplementary Figure 7. Outline of breeding crosses for Sleeping Beauty mutagenesis studies. For details, see Takeda et al. *Nature Genetics*. 2015.

	Forward Sequence	Reverse Sequence	Citation/ PrimerBank ID
Axin2	TGACTCTCCTTCCAGATCCCA	TGCCCACACTAGGCTGACA	31982733a1
cMyc	ATGCCCCTCAACGTGAACTTC	GTCGCAGATGAAATAGGGCTG	293629266c1
Lgr5	CCAATGGAATAAAGACGACGGCAACA	GGGCCTTCAGGTCTTCCTCAAAGTCA	Jaks et al. *Nat Genet*. 2008
Cdh1	CCAACAGGGACAAAGAAACAAAGG	GATGACACGGCATGAGAATAGAGG	Slorach et al. *Genes Dev*. 2011
Ctnna1	GCCAAGCAGATGTGCATGATC	CAGAGGTGTTTTTGAGTGGACCTT	Slorach et al. *Genes Dev*. 2011
Ctnnb1	GGGTGGCATAGAGGCTCTTGT	GCTCAGTGATGTCTTCCCTGTCA	Slorach et al. *Genes Dev*. 2011
Ctnnd1	AGCTTGTGGAGAATTGTGTTTGC	TGCCTGTGGGATTTCACGAT	Slorach et al. *Genes Dev*. 2011
Zbtb33	GAACTCCTTGAATGAACAGCGT	CCCAGCAACTGAGAAGAGC	9937986a1
Gapdh	TGACCTCAACTACATGGTCTACA	CCGTGAGTGGAGTCATACTGG	

Supplemental Table 2. Primer sequences for qRT-PCR analysis. Primers not previously cited were designed using NCBI-GENE-'Pick Primers' function. Primer sequences obtained through the PrimerBank database (Massachusetts General Hospital) are identified according to their PrimerBank ID numbers.